PHYSICAL REVIEW E **69**, 016409 (2004)

Equation of state and transport coefficients for dense plasmas

C. Blancard and G. Faussurier
Département de Physique Théorique et Appliquée, CEA/DAM Ile-de-France, Boîte Postale 12, F 91680 Bruyères-le-Châtel, France

(Received 17 September 2003; published 30 January 2004)

We hereby present a model to describe the thermodynamic and transport properties of dense plasmas. The electronic and ionic structures are determined self-consistently using finite-temperature density functional theory and Gibbs-Bogolyubov inequality. The main thermodynamic quantities, i.e., internal energy, pressure, entropy, and sound speed, are obtained by numerical differentiation of the plasma total Helmholtz free energy. Electronic electrical and thermal conductivities are calculated from the Ziman approach. Ionic transport coefficients are estimated using those of hard-sphere system and the Rosenfeld semiempirical ''universal'' correspondence between excess entropy and dimensionless transport coefficients of dense fluids. Numerical results and comparisons with experiments are presented and discussed.

DOI: 10.1103/PhysRevE.69.016409 PACS number(s): 52.25.Kn, 52.27.Gr

I. INTRODUCTION

Early theoretical study of matter at high density and high temperature was aimed at understanding pressure balance and energy flow in stellar interiors [1]. Since the 1980s, there has been a growth of interest in the atomic properties of hot dense plasmas, motivated by laboratory experiments involving high-power pulsed lasers. More recently, the interest has been enhanced by the possibility of producing plasmas near solid density and at temperatures in the range 0.1–1 keV with ultrashort duration laser pulse. Some experiments have also been carried out to measure the electrical resistivity [2–4] or the optical reflectivity [5,6] of strongly coupled plasmas [7]. In this field, combined pressure, electrical resistivity, and internal energy variation measurements of warm dense aluminum and titanium plasmas have been recently performed [8,9].

Though much is known about the equation of state and transport coefficients for most materials under many conditions [10], there are domains where common theories are questionable or way out of their range of validity [11,12]. This is typically the case for strongly coupled plasmas in the density-temperature plane between solid and plasma called warm dense matter [13]. This equilibrium thermodynamic regime can be encountered in planetary interiors, cool dense stars, and in laboratory experiments. The knowledge of equation of state of such strongly coupled plasmas, characterized by Coulomb potential energy between plasma particles greater than their average kinetic energy, is therefore crucial and challenging. But this task is extremely difficult to achieve due to the complex and subtle coupling between ionic and electronic structures. Indeed, any model that is supposed to describe dense plasmas, and warm dense matter in particular, should solve the following problems [14]. It should be able to calculate the average electron-density profile around an ion in the plasma, determine a self-consistent average ionization of the plasma, compute the interaction between ions, the total Helmholtz free energy of the plasma, and the largest possible set of ionic and electronic transport coefficients. It should also be valid in the high-density and high-temperature domain where the Thomas-Fermi approach is known to work well [15], and be robust enough to ensure a transition, as smooth and physically correct as possible, with solid state physics [16]. Moreover, it should be *ab initio* and have a high degree of intrinsic consistency. Finally, its design should be flexible and modular enough in order to be easily improved and modified through the implementation of new physics without having to build another model from scratch. Clearly, the model should get rid of the standard simplified descriptions of ionic distribution (isolated ion sphere, uniform positive background, perturbation theory, pseudopotential approach, and linear response theory, . . .). This is the cornerstone of the whole issue. The description of dense plasmas is a nonlinear and coupled problem, in which it is acknowledged that neglecting altogether the details of ion correlations and their effect on the thermodynamics of the model will one day lead to failure, one way or another. Indeed, the ionic contribution to the equation of state is understood to be relatively small in itself, especially in high-Z materials, and when compared with the electronic part. However, their indirect influence in providing boundary conditions for the electronic equations can be much more significant, and may have an important impact due to the strong lever arm effect [17].

This document presents a first-principles approach that provides some answers to the aforementioned problems. Our model is based on the neutral pseudoatom (NPA) concept [18]. This means that the plasma can be considered as an effective classical system of virtual neutral particles, i.e., a collection of NPA interacting via an interatomic effective pair potential Φ. Electrons of the NPA satisfy a Schrödinger equation with an effective potential V_{eff}. V_{eff} and Φ expressions are established using a variational principle based on the Gibbs-Bogolyubov inequality (GBI) [19]. This means that we find the best one-electron Hamiltonian, in the sense of the Gibbs-Bogolyubov inequality, i.e., the best NPA one-electron density, to represent the original many-body Hamiltonian of the overall electron and bare nucleus neutral system [20]. Both V_{eff} and Φ are determined by the electronic structure and the ionic distribution of the plasma. In order for the model to be computationally tractable, the density functional theory (DFT) within the local density approximation (LDA) is used to estimate the exchange-correlation effects, and the Gibbs-Bogolyubov inequality is again employed to look for

1063-651X/2004/69(1)/016409(15)/$22.50

the best reference system, i.e., one component plasma (OCP) or hard-sphere (HS) systems, to get the pair distribution function of the ionic subsystem from the interatomic effective potential Φ [21–23]. In Sec. II, the general formalism is proposed. Mathematical details and additional developments are given in the appendixes. Numerical results and comparisons to measurements are presented in Sec. III. Section IV is the conclusion.

II. FORMALISM

In this section, we derive the expression of the total free energy of the plasma using finite-temperature density functional theory, within the local density approximation, and the powerful variational approach based on the Gibbs-Bogolyubov inequality. Viewing the plasma as a collection of identical neutral pseudoatoms, the variational method enables one to find the optimum one-electron Hamiltonian that gives the best approximation of the original many-body total Hamiltonian of the plasma. We thus naturally find the expressions of the effective electron-ion and ion-ion potentials that describe the electron-ion and ion-ion interactions inside the system. The NPA electronic structure is found solving a Schrödinger equation with the relevant effective electron-ion potential. The ionic structure is found using the GBI to establish a mapping between the effective ion-ion system and the hard-sphere or the one-component plasma reference systems. The knowledge of the total free energy of the plasma gives access to the main thermodynamic quantities of interest by numerical differentiation. We then assume that the Ziman formalism can be used to calculate the electronic electrical and thermal conductivities of the system. We also provide a means of estimating ionic transport coefficients from either the Rosenfeld semiempirical "universal" corresponding-state relationships based on the reduced configurational entropy, or simply using the reference system transport coefficients.

A. Derivation of the total free energy of the system

Let us consider a plasma containing N_I nuclei of nuclear charge Z_I of a single element and $N_I Z_I$ electrons in a volume *V*. The whole system is supposed to be neutral, homogeneous, isotropic, and in thermodynamic equilibrium at temperature *T*. The ion density $\rho_I = N_I/V$ is related to the Wigner-Seitz radius a_{WS} by the standard formula $(4\pi/3)a_{WS}^3\rho_I = 1$. $1/\rho_i$ is the volume occupied by one nucleus. Inverse temperature β is equal to $1/k_BT$, where k_B is the Boltzmann constant. The Hamiltonian of this system is written as follows:

$$H_{sys} = \sum_j \frac{\mathbf{P}_j^2}{2M} + V_{II} + H_e\,, \tag{1}$$

where V_{II} is the bare nucleus Coulomb potential, i.e.,

$$V_{II} = \sum_{i>j} \frac{Z_I^2 e^2}{|\mathbf{R}_i - \mathbf{R}_j|}, \tag{2}$$

and H_e the electron Hamiltonian, i.e.,

$$H_e = \sum_j \frac{\mathbf{p}_j^2}{2m} + \sum_{i>j} \frac{e^2}{|\mathbf{r}_i - \mathbf{r}_j|} - \sum_{i,j} \frac{Z_I e^2}{|\mathbf{r}_i - \mathbf{R}_j|}. \tag{3}$$

$M(m),\mathbf{P}(\mathbf{p})$ are nucleus (electron) mass and momentum, respectively. $\mathbf{R}(\mathbf{r})$ is the nucleus (electron) vector radius. The nucleus (electron) indices run between 1 and N_I $(Z_I N_I)$. When there is no ambiguity, the sum limits will be made implicit for conciseness.

We invoke the Born-Oppenheimer approximation, in which the nuclear and electronic motions are separated. We can treat the electrons quantum mechanically and the nuclei classically. In other words, the time scale that is necessary for electrons to adapt to a nucleus configuration change under the influence of internal forces is much shorter than the time scale required for nuclei to go from one configuration to another one under the influence of the same forces. This approximation is also known as the adiabatic approximation. We can thus integrate out the electronic coordinates apart from the nuclear ones, i.e., the trace over the electronic degrees of freedom must be performed assuming a given and fixed nucleus configuration. Of course, one must then trace over the nucleus degrees of freedom to arrive at the final statistical average of the observable of interest. From the electronic point of view, the third term of the right-hand side of Eq. (3) acts as an external potential due to the electrostatic interaction between electrons and nuclei. From the nucleus viewpoint, the trace over the electronic degrees of freedom eliminates the direct two-body electrostatic interaction between electrons and nuclei, and produces an effective indirect interaction between nuclei. The nuclei can thus be seen as a classical gas of particles interacting through pairwise electrostatic interaction and immersed in an external field that causes them to interact through an effective many-body interaction. As a result, the quantum mechanical electron problem is solved using purely classical forces. However, since electrons must obey the Pauli exclusion principle, i.e., satisfy Fermi-Dirac statistics, the classical mechanical nucleus problem is solved using both classical and quantum forces. To sum up, starting from a two-component system, i.e., electrons and nuclei, it is possible to reduce the original problem to a one-component plasma by eliminating electronic degrees of freedom. Yet the underlying electron presence manifests itself through the effective many-body interaction, which adds to the electrostatic interaction between nuclei. Then, depending on the nature of material and on thermodynamic conditions, we could face an amazing and huge diversity of physical situations and phenomena.

We propose an *ab initio* model to describe self-consistently the electronic and ionic structures of plasmas. This approach should be in agreement with the Thomas-Fermi theory at high density and should give a reasonable matching with the methods originally developed to describe low-temperature condensed matter, i.e., methods based on pseudopotential and perturbation theories or quantum molecular dynamics approaches. Of course, comparisons with relevant and discriminant experiments are essential for testing the overall theoretical framework. So, returning to Eqs.

(1)–(3), our main problem is to choose a simple, robust, predictive, and computationally tractable strategy to eliminate the electronic degrees of freedom, in order to achieve the reduction of our system to a one-component plasma. The most natural idea involves using the fruitful approach employed frequently in various fields such as atomic physics, molecular physics, or nuclear physics, i.e., to look for the best one-electron Hamiltonian $\hat{H}_{e0}$ using the GBI. Our approach, based on a seminal paper by Kiyokawa [20], is very different from the NPA approach enhanced by Perrot [14], which involves extending the solid- and liquid-state models to plasmas. This method has been shown to lead to a consistent treatment of the high-temperature fluid phase. However, Perrot's method is not variational but perturbative, and its validity is warranted only if the electronic structure is "simple," in the sense of the simple liquid-metal theory. It is rather delicate to estimate the influence of the neglected terms in the free energy expansion. Moreover, as stated by the author, complex effects such as molecular- or cluster-level formation, which involve charge redistribution and three (or more) ion interactions cannot be dealt with. This is not the case with our approach, which can be refined to enrich the physical description, if needed.

As is usually the case in statistical mechanics, we have to decide in which ensembles we are going to treat the N_I nuclei and the $N_I Z_I$ electrons. Since in the thermodynamic limit, i.e., $N_I \to \infty$, $V \to \infty$, $N_I/V = \rho_I = \text{const}$, results do not depend on a particular choice, let us choose ensembles that lead to simple and convenient calculations, and which seem close to the physical properties of the systems of interest. According to the adiabatic approximation, it seems normal to treat the N_I slow nuclei in the canonical ensemble and the fast $N_I Z_I$ electrons in the grand canonical ensemble. Let us introduce the nuclear chemical potential μ_I, the electron chemical potential μ_e, and the electron number operator $\hat{N}_e$. Since electrons are treated quantum mechanically, H_{sys} and H_e become operators and should be read $\hat{H}_{sys}$ and $\hat{H}_e$, respectively. The grand potential of the system Ω_{sys} is equal to

$$e^{-\beta\Omega_{sys}} = e^{\beta\mu_I N_I}\,\mathrm{Tr}[e^{-\beta(\hat{H}_{sys}-\mu_e\hat{N}_e)}], \tag{4}$$

where Tr means trace over electronic and nuclear degrees of freedom. As for electrons, the trace is performed over the complete Fock space and is noted Tr_e, whereas for nuclei, the trace is referred to as Tr_I and simply read as

$$\mathrm{Tr}_I\{\cdots\} = \int \frac{d^{N_I}\mathbf{R}\,d^{N_I}\mathbf{P}}{N_I!\,h^{3N_I}}\{\cdots\}, \tag{5}$$

where h is the Planck constant. Using the adiabatic approximation, Eqs. (1)–(3), and remembering that the nuclear quantities are usual numbers that commute with electron operators,

$$e^{-\beta\Omega_{sys}} = e^{\beta\mu_I N_I}\,\mathrm{Tr}_I\Bigg\{\exp\left(-\frac{\beta}{2M}\sum_j \mathbf{P}_j^2 - \beta V_{II}\right) \times \mathrm{Tr}_e[e^{-\beta(\hat{H}_e-\mu_e\hat{N}_e)}]\Bigg\}. \tag{6}$$

The integrations over nuclear momenta can be carried out explicitly, yielding a factor $(2\pi M k_B T)^{1/2}$ for each degree of freedom. Introducing the nuclear de Broglie thermal wavelength $\Lambda = (2\pi\beta\hbar^2/M)^{1/2}$ and the free energy F_I^{id} of a perfect gas,

$$e^{-\beta F_I^{id}} = \int \frac{d^{N_I}\mathbf{R}\,d^{N_I}\mathbf{P}}{N_I!\,h^{3N_I}}\exp\left(-\frac{\beta}{2M}\sum_j \mathbf{P}_j^2\right) = \frac{V^{N_I}}{\Lambda^{3N_I}N_I!}, \tag{7}$$

we obtain a more compact equation

$$e^{-\beta\Omega_{sys}} = e^{-\beta F_I^{id}+\beta\mu_I N_I}\,\mathrm{tr}_I\{e^{-\beta V_{II}}\,\mathrm{Tr}_e[e^{-\beta(\hat{H}_e-\mu_e\hat{N}_e)}]\}. \tag{8}$$

In this expression, symbol "id" stands for ideal and tr_I is a shorthand notation for

$$\mathrm{tr}_I\{\cdots\} = \int \frac{d^{N_I}\mathbf{R}}{V^{N_I}}\{\cdots\}. \tag{9}$$

Now, let us find a lower bound to $e^{-\beta\Omega_{sys}}$ using $\hat{H}_{e0}$ and the GBI. Inserting $\pm\hat{H}_{e0}$ near $\hat{H}_e$ in Eq. (8), using

$$\langle\{\cdots\}\rangle_{e0} = \frac{\mathrm{Tr}_e[e^{-\beta(\hat{H}_{e0}-\mu_e\hat{N}_e)}\{\cdots\}]}{e^{-\beta\Omega_{e0}}},$$

$$e^{-\beta\Omega_{e0}} = \mathrm{Tr}_e[e^{-\beta(\hat{H}_{e0}-\mu_e\hat{N}_e)}], \tag{10}$$

and the well-known property

$$\langle e^{-\beta(\hat{H}_e-\hat{H}_{e0})}\rangle_{e0} \geqslant e^{-\beta\langle\hat{H}_e-\hat{H}_{e0}\rangle_{e0}}, \tag{11}$$

we naturally find that

$$e^{-\beta\Omega_{sys}} \geqslant e^{-\beta F_I^{id}+\beta\mu_I N_I}\,\mathrm{tr}_I[e^{-\beta V_{II}-\beta\Omega_{e0}-\beta\langle\hat{H}_e-\hat{H}_{e0}\rangle_{e0}}]. \tag{12}$$

Now, let us determine what kind of trial one-electron Hamiltonian we use. In general, some electrons in the system are localized in the neighborhood of a nucleus or cluster of nuclei and occupied bound states. The others are in continuum states. However, let us leave bound states of cluster to one side, i.e., molecularlike orbits in the present work. This is our first assumption. In other words, there is no overlap of eigenfunctions between two different atomic sites. The electrons of the system that are trapped and tightly attached to nuclei are called bound electrons. The other electrons that move in the whole space or belong to all nuclei are called delocalized or free electrons. We define an ion as the system consisting of one nucleus and some bound electrons belonging to it. However, the density profile of the continuum electrons is not stationary due to the nucleus motion. So, these electrons tend to pile up near the nuclei in the sense of the adiabatic approximation, and shield or screen the ionic charges. Therefore, it is physically reasonable to consider the system comprising an ion plus the part of the continuum electrons, which helps to shield that particular ionic charge, such as an "atom," i.e., a neutral atomic system. Though this particular ion will not be screened by the same continuum electrons during its motion, there will be a fraction of the free electrons that will shield this particular ion on average, in the sense of the statistical mechanics. So, it seems possible to consider a plasma as being constructed by such virtual atoms or neutral pseudoatoms. We come thus naturally to our second assumption that all atoms in the system have the same electronic structure. This means that we do not yet discriminate the different charge stages of the plasma. Consequently, we introduce the following unperturbed Hamiltonian operator:

$$\hat{H}_{e0}=\sum_{j}\sum_{n}\varepsilon_{n}\hat{\mathbf{a}}_{jn}^{\dagger}\hat{\mathbf{a}}_{jn}, \tag{13}$$

where $\hat{\mathbf{a}}_{jn}^{\dagger}$ and $\hat{\mathbf{a}}_{jn}$ are creation and annihilation operators acting on quantum state n in the jth ion and satisfy the anticommutation relations (A5) and (A6) in Appendix A. Equation (A5) means that two electrons are independent of each other when the first electron is in one ion and the second is in another ion. Since we suppose that neutral pseudoatoms do not interact with each other, the trial one-electron energy ε_n does not depend on label j. Neglecting relativistic effects, one-electron wave function $\varphi_n(\mathbf{r})$ and energy ε_n are solutions of a Schrödinger equation with a central symmetric effective potential $v_{eff}(\mathbf{r})$:

$$\left[-\frac{\hbar^2\nabla^2}{2m}+v_{eff}(\mathbf{r})\right]\varphi_n(\mathbf{r})=\varepsilon_n\varphi_n(\mathbf{r}). \tag{14}$$

The trial potential $v_{eff}(\mathbf{r})$ must be determined self-consistently but is still unknown at the stage of this work. Once chosen $\hat{H}_{e0}$, the thermal average of the Hamiltonian $\hat{H}_e$, written in the second-quantification formalism, can be performed using the eigenstates of $\hat{H}_{e0}$; both Ω_{e0} and $\langle\hat{H}_e-\hat{H}_{e0}\rangle_{e0}$ can be obtained in closed form. The derivation is detailed in Appendix A. The final result reads

$$\begin{aligned}\langle\hat{H}_e-\hat{H}_{e0}\rangle_{e0}=&N_I\left[E_X(0)-\frac{e^2}{2}\int\int\frac{\rho_e(\mathbf{r})\rho_e(\mathbf{r}')}{|\mathbf{r}-\mathbf{r}'|}d\mathbf{r}d\mathbf{r}'\right]\\&+N_I\left[\int\rho_e(\mathbf{r})v_{at}(\mathbf{r})d\mathbf{r}-\int\rho_e(\mathbf{r})v_{eff}(\mathbf{r})d\mathbf{r}\right]\\&+\frac{1}{2}\sum_{i\neq j}\left[-\frac{Z_I^2e^2}{|\mathbf{R}_{ji}|}+\Phi(\mathbf{R}_{ji})\right]\end{aligned} \tag{15}$$

and

$$\Omega_{e0}=-\frac{N_I}{\beta}\sum_n \ln[1+e^{-\beta(\varepsilon_n-\mu_e)}], \tag{16}$$

where

$$v_{at}(\mathbf{r})=-\frac{Z_Ie^2}{|\mathbf{r}|}+e^2\int\frac{\rho_e(\mathbf{r}')}{|\mathbf{r}-\mathbf{r}'|}d\mathbf{r}', \tag{17}$$

and

$$\Phi(\mathbf{R})=2E_X(\mathbf{R})-Z_Iv_{at}(\mathbf{R})+\int\rho_e(\mathbf{r})v_{at}(\mathbf{r}-\mathbf{R})d\mathbf{r}. \tag{18}$$

The NPA electronic density $\rho_e(\mathbf{r})$ is equal to

$$\rho_e(\mathbf{r})=\sum_n f_n|\varphi_n(\mathbf{r})|^2, \tag{19}$$

where

$$f_n=\frac{1}{1+e^{\beta(\varepsilon_n-\mu_e)}}, \tag{20}$$

and with

$$\int\rho_e(\mathbf{r})d\mathbf{r}=Z_I \tag{21}$$

to ensure charge conservation. This is accomplished by adjusting the electronic chemical potential μ_e. $E_X(\mathbf{R})$ is the exchange energy coming from two groups of electrons belonging to different ions, one placed at the origin and the other at $\mathbf{R}$. What is important to note is the precise cancellation of the bare nuclear electrostatic interaction V_{II} due to screening. Indeed, the one-electron Hamiltonian $\hat{H}_{e0}$, where the overlap of eigenfunctions between two different atomic sites is neglected, naturally induces an effective two-body ion-ion potential $\Phi(\mathbf{R}_{ji})$ depending on the relative distance between ions i and j. Moreover, these are the only terms that are functions of nucleus positions due to the effective separation between ionic and electronic degrees of freedom. Inserting Eqs. (15) and (16) inside Eq. (12), the trace over nucleus positions only concerns terms involving the effective ion-ion potential. This multidimensional integral has a very clear physical interpretation. From the theory of simple liquids [22], we know that

$$\mathrm{tr}_I\left[\exp\left(-\frac{\beta}{2}\sum_{i\neq j}\Phi(\mathbf{R}_{ji})\right)\right]=e^{-\beta F_\Phi^{ex}}, \tag{22}$$

where F_Φ^{ex} is the excess free energy of the system of N_I ions interacting via the pairwise effective interaction potential $\Phi(\mathbf{R})$. We thus find the expression on which the GBI will be applied,

$$\frac{\Omega_{sys}}{N_I}\leqslant\Omega_I+\Omega_e, \tag{23}$$

where Ω_I and Ω_e may be interpreted as the ionic and electronic contributions to the grand potential per nucleus, i.e.,

$$\Omega_I=\frac{F_I^{id}}{N_I}+\frac{F_\Phi^{ex}}{N_I}-\mu_I \tag{24}$$

and

$$\Omega_e = -\frac{1}{\beta}\sum_n \ln[1+e^{-\beta(\varepsilon_n-\mu_e)}]+E_X(0) - \frac{e^2}{2}\int\int \frac{\rho_e(\mathbf{r})\rho_e(\mathbf{r}')}{|\mathbf{r}-\mathbf{r}'|}d\mathbf{r}d\mathbf{r}' + \int \rho_e(\mathbf{r})v_{at}(\mathbf{r})d\mathbf{r} - \int \rho_e(\mathbf{r})v_{eff}(\mathbf{r})d\mathbf{r}. \tag{25}$$

At this stage, we have a relatively compact expression for the grand potential of the system Ω_{sys}, in which the only unknown is the NPA electronic density ρ_e. Once determined, so are the effective potential v_{eff}, the electronic contribution Ω_e, and the effective ion-ion potential, but not the excess free energy F_Φ^{ex}. This is a serious and crucial drawback because we need to know this quantity to calculate the total free energy of the system, and by extension, the bulk equation of state. This delicate question has been a recurrent and difficult task for many years in the theory of simple liquids [21,22]. The simplest strategy is to apply the GBI to the ionic contribution F_Φ^{ex} too. Though many systems can be used as reference systems, the number of choices is drastically reduced if we take into account the constraints that such a reference system should obey in order to test the GBI efficiently. We must have access to the excess free energy, the excess internal energy, and the radial pair-correlation function over the entire fluid domain. Moreover, the main transport coefficients, i.e., self-diffusion, shear viscosity, and thermal conductivity, must be known analytically in the same conditions. To our knowledge, the HS and the OCP systems are the only many-body systems that can pass this test and can be selected as two possible reference systems [23]. Let us denote $F_{ref}^{ex}(\lambda)$, $U_{ref}^{ex}(\lambda)$, $g_{ref}(\lambda,\mathbf{R})$, and $\Phi_{ref}(\lambda,\mathbf{R})$ the excess free energy, the excess internal energy, the radial pair distribution function, and the pair potential of the reference system. We assume that this reference system can be described by a generic parameter λ. Extension to many parameter case raises no problem. As shown in Appendix B, the GBI applied this time to F_Φ^{ex} leads to

$$F_\Phi^{ex} \leqslant F_{ref}^{ex}(\lambda) - U_{ref}^{ex}(\lambda) + \frac{N_I\rho_I}{2}\int g_{ref}(\lambda,\mathbf{R})\Phi(\mathbf{R})d\mathbf{R}. \tag{26}$$

Care must be taken when a OCP system is employed due to the neutralizing background always implicitly assumed for this kind of system. So, we have an upper bound to Ω_I using this inequality. Finally,

$$\frac{\Omega_{sys}}{N_I} \leqslant \frac{F_I^{id}+F_{ref}^{ex}(\lambda)-U_{ref}^{ex}(\lambda)}{N_I} + \frac{\rho_I}{2}\int g_{ref}(\lambda,R)\Phi(\mathbf{R})d\mathbf{R} - \mu_I + \Omega_e. \tag{27}$$

Introducing the total free energy per NPA of the system F_{tot} as

$$F_{tot} = \frac{F_I^{id}+F_{ref}^{ex}(\lambda)-U_{ref}^{ex}(\lambda)}{N_I} + \frac{\rho_I}{2}\int g_{ref}(\lambda,R)\Phi(\mathbf{R})d\mathbf{R} + \Omega_e + Z_I\mu_e, \tag{28}$$

the GBI for ions (electrons) says that F_{tot} is minimum for any variation of λ (ρ_e) at fixed T, N_I, Z_I, V, and ρ_e (λ). As shown in Appendix C,

$$\frac{\partial F_{tot}}{\partial \lambda} = 0 \tag{29}$$

leads to

$$\frac{\rho_I}{2}\int \frac{\partial g_{ref}(\lambda_{eff},\mathbf{R})}{\partial \lambda}[\Phi(\mathbf{R}) - \Phi_{ref}(\lambda_{eff},\mathbf{R})]d\mathbf{R} = 0, \tag{30}$$

whereas

$$\frac{\delta F_{tot}}{\delta \rho_e(\mathbf{r})} = 0 \tag{31}$$

leads to

$$v_{eff}(\mathbf{r}) = v_{at}(\mathbf{r}) + \frac{\delta E_X(0)}{\delta \rho_e(\mathbf{r})} + \rho_I\int \left[v_{at}(\mathbf{r}-\mathbf{R}) + \frac{\delta E_X(\mathbf{R})}{\delta \rho_e(\mathbf{r})}\right] \times g_{ref}(\lambda,\mathbf{R})d\mathbf{R}. \tag{32}$$

Equations (30) and (32) determine the effective parameter λ_{eff} of the reference ionic system and the effective electron-ion potential v_{eff}, respectively. Equation (30) is rather standard. Equation (32) needs some comments. The electrostatic part results in a simple charge superposition. This means that to calculate the electrostatic potential at a given radius, we only need to add the electrostatic potential of the NPA located at the origin and the electrostatic potential of the other NPA of the plasma, with the conditional probability that there is a NPA at the origin, hence the presence of the pair distribution function $g_{ref}(\lambda,\mathbf{R})$. The exchange contribution is more complicated to interpret, except if we consider the DFT in the LDA, where a similar conclusion may be drawn using the exchange potential. Indeed, this exchange contribution is also the most delicate one to calculate, simply for computational time reasons. As for electrons, we have adopted the numerical schemes of the DFT in the LDA proposed by Iyetomi and Ichimaru [24] at finite temperature and by Perdew and Wang [25] at zero temperature. These schemes have been implemented after intensive comparisons with experiments. As for consistency, we have kept the same approach for ions using the Gordon and Kim [26] method to estimate the exchange contribution within the effective ionic pair potential.

The whole equations obtained up to now are exact in the sense of the variational GBI method using the trial one-electron Hamiltonian H_{e0} and the reference ionic system. One understands that choosing both other H_{e0} and reference ionic systems to improve the description of physics will lead to different equations but the cornerstone of the formalism, i.e., the GBI approach, remains the same. It is very interesting and encouraging, because one does not have to change the complete theoretical formalism to add new effects, if we keep the GBI method of course. Assumptions have been clearly enhanced; improvements are easily localizable, but this does not mean that their implementations are straightforward. However, as already apparent here, two main problems will quickly arise, i.e., the mapping between the effective ion-ion potential and the pair distribution function that allows the calculation of the ionic part of the free energy and the question of exchange and correlation. Before improving physics with the inclusion of new effects, we think that we must keep in mind the two aforementioned difficulties, in order to obtain computationally tractable equations to compare to experiment. This can be done either for equation of state or transport coefficients.

B. Equation of state

The entire formalism presented up to now has been implemented in the SCAALP model in order to describe the microscopic properties of dense media. Once the NPA electronic density ρ_e and the effective parameter λ_{eff} of the ionic reference system have been determined, it is a simple task to calculate the total free energy of the system F_{tot} using Eqs. (25) and (28). Nearly the whole thermodynamic quantities of interest may be obtained by simple differentiation of F_{tot} with respect to temperature T and volume V (or mass density ρ). For instance, internal energy U, pressure P, and entropy S are given by the standard expressions

$$U=F_{tot}-T\left.\frac{\partial F_{tot}}{\partial T}\right|_V=\left.\frac{\partial(\beta F_{tot})}{\partial \beta}\right|_V,$$

$$P=\left.\frac{\partial F_{tot}}{\partial V}\right|_T,$$

$$S=-\left.\frac{\partial F_{tot}}{\partial T}\right|_V. \tag{33}$$

Another very important quantity is sound speed c_S, which can be calculated from the formula

$$c_S=\sqrt{\left.\frac{\partial P}{\partial \rho}\right|_T+\frac{(\partial S/\partial \rho)|_T}{(\partial S/\partial T)|_\rho}\left.\frac{\partial P}{\partial T}\right|_\rho}. \tag{34}$$

Indeed, since our model is thermodynamically self-consistent, we know that internal energy U and pressure P satisfy the fundamental equation

$$\left.\frac{\partial U}{\partial V}\right|_T=T\left.\frac{\partial P}{\partial T}\right|_V-P. \tag{35}$$

A large amount of work has been done to solve numerically the self-consistent mean-field equations of the SCAALP model in order to respect Eq. (35). This is achieved by the severe constraints concerning the convergence parameters and the use of Chebyshev polynomials [27]. It can be seen that any model incapable of passing this test is definitely incorrect.

C. Transport coefficients

Transport coefficients such as self-diffusion, viscosity, thermal conductivity, or electrical conductivity are the most fundamental dynamical parameters that reflect the nature of the interparticle potentials and characterize the thermodynamics of the system. A theory developed to describe the bulk thermodynamic equilibrium properties is not usually guaranteed to be particularly capable of predicting dynamic properties of systems, such as transport coefficients. Since in our model, ions form a classical system of particles interacting via an effective pairwise potential Φ, we could use classical molecular dynamics as a postprocessor to estimate transport coefficients using well-known techniques from simple liquid theory. However, following recent studies made on the Yukawa one-component plasma (YOCP) system, we estimate the self-diffusion, the shear viscosity, and the thermal conductivity of dense plasmas from the transport coefficients of the ionic reference system (HS or OCP) [23]. Moreover, we also recommend the use of the elegant method proposed by Rosenfeld, which relates the transport coefficients to the equation of state [28,29]. This approach consists of using a semiempirical universal corresponding-state relationship, for the dimensionless transport coefficients of dense fluids as functions of the reduced configurational entropy. The same author has extended this technique to dilute fluids, established by many simulations. The Rosenfeld approach is powerful for many reasons. First, an accurate, theoretically based approach to dense-fluid transport coefficients is still lacking. Second, no convergent perturbation theory of transport coefficients has been established. Third, the brute-force computer methods can be used to estimate transport coefficients, but these methods are considerably too time consuming, for the same accuracy, than those designed to measure equilibrium properties and cannot be considered as black-box routines. Fourth, this analytical relation between transport coefficients and excess entropy allows us to estimate, for instance, self-diffusion, shear viscosity, and thermal conductivity from the equation of state of monoatomic fluids with arbitrary pair potentials. In summary, one realizes all the benefits of the Rosenfeld approach to estimate transport coefficients knowing only the excess entropy of the system of interest. This method is as useful as Enskog's original recipe relating transport coefficients to thermal pressure. Details and the whole formulas of interest can be found in Ref. [23], where such methods have been extensively applied and discussed.

Many and well-characterized experiments using either exploded wires or isochoric plasma closed vessel have been performed for electrical resistivity. Since in these regimes, electrical conduction mostly originates from electrons, we consider it interesting and valuable to calculate also electronic electrical resistivity with the SCAALP model. The simplest plasma resistivity calculations use the Spitzer formula, which make use of many simplifying assumptions, such as the Saha theory in hot plasma physics. Some other approaches have been proposed to calculate resistivity for any kind of plasmas. However, most of these models were intended to facilitate on-line hydrocode calculations. Since we are rather interested in an *ab initio* and microscopic approach, we have adopted the extension of the Ziman formula to finite temperature. Our method is similar to the one proposed by Perrot and Dharma-wardana [30,14]. This method has been discussed at length so we will not elaborate any further. Any readers who are interested should consult the original papers. Indeed, results obtained with this method should be considered as a good first approximation requiring further corrections depending on specific experimental conditions. Since the Ziman formula corresponds to the simplest variational solution of a transport equation, higher-order terms arising from other basis functions become important in certain problems. This must be the case, for instance, for nearly neutral plasmas where the Ziman formula is expected to be too rustic in such conditions. Calculating some other linear transport properties, such as thermal conductivity, is then simple to carry out and will not be considered here [18].

III. COMPARISONS TO EXPERIMENT

In this section, we test the accuracy of the SCAALP model by comparing its predictions to experimental results. We have chosen to concentrate first on aluminum. Many experimental data concerning equation of state (EOS) quantities and electronic electrical conductivity are available for this simple metal. Its EOS is often considered to be an accurate standard for EOS studies. However, the exact evaluation of thermodynamic properties may be very difficult to obtain, even for such a ‘‘simple’’ material [12]. From a theoretical point of view, no theory exists that can describe the bulk properties over the entire temperature-density plane. The Sesame EOS for aluminum consists, for instance, in a patchwork of subregions covered by various theories. There is an area which is not addressed by any theory. It is only accessed by numerical interpolation from the adjacent regions where data are available. The ‘‘unknown’’ area, roughly defined by $0.1<\rho<2\ \mathrm{g\,cm^{-3}}$ and $1<T<50\ \mathrm{eV}$, is such that the plasma is strongly coupled [11]. For aluminum, this area belongs to the warm dense matter field. This is a regime between solid and plasma, where the description of physics is complicated due to the strong interaction between particles, i.e., ions and electrons. It is only recently that experimental data become available in order to validate calculations in these particular thermodynamic conditions.

The SCAALP model is tested first in the cold dense regime relevant to solid state physics. Of course, our model, designed to describe the properties of plasmas, is not expected to give an accurate description of bulk properties in this domain. However, it is interesting to see how SCAALP behaves when it progressively leaves its domain of validity, i.e., decreasing temperature to go from plasma to solid. We have plotted in Fig. 1 the cold compression curve considering SCAALP and three other theories of increasing accuracy, i.e., quotidian equation of State (QEOS) [31], embedded atom model (EAM) [32], and all electron method [33,34], respectively. Experimental data points [35,36] are also given. We see that the overall behavior of SCAALP is good. The excellent agreement at high compression with TFD was expected to prevail *a priori* but the fair agreement with solid state physics, i.e., EAM or all electron model at low density, is rather encouraging. This indicates that we may be confident concerning the predictions of the SCAALP model in the boundary domain between solid state physics and plasma physics.

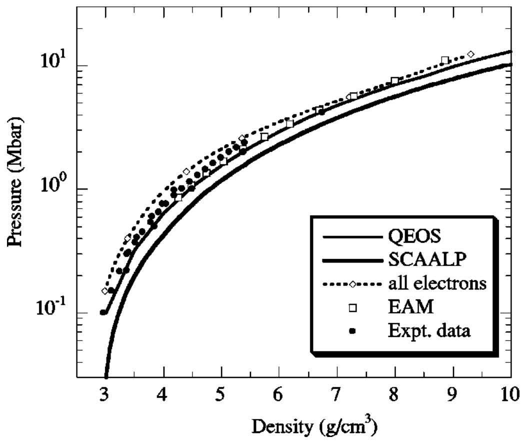

FIG. 1. Aluminum cold compression curve considering SCAALP, Quotidian equation of state (QEOS) [31], embedded atom model (EAM) [32], all electron method [33,34], and experimental data points [35,36].

The aluminum equation of state at high pressure is investigated with SCAALP by calculating the Hugoniot curve starting from normal condition of temperature and pressure, i.e., 300 K and solid density. The Hugoniot curve obtained with the SCAALP model is compared to Sesame, QEOS, and experimental data [37] in Fig. 2. We can see that SCAALP results are as accurate as EOS data table and semiempirical models. Moreover, they emphasize the thermodynamic domain where the Hugoniot curve strongly depends on electronic structure, i.e., beyond four times solid density where

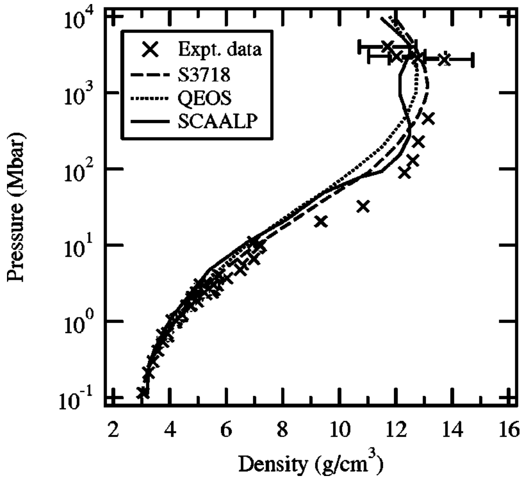

FIG. 2. Aluminum Hugoniot predictions using SCAALP, Quotidian equation of state (QEOS) [31], and Sesame [10,11] (S3718) are compared to experimental data [37].

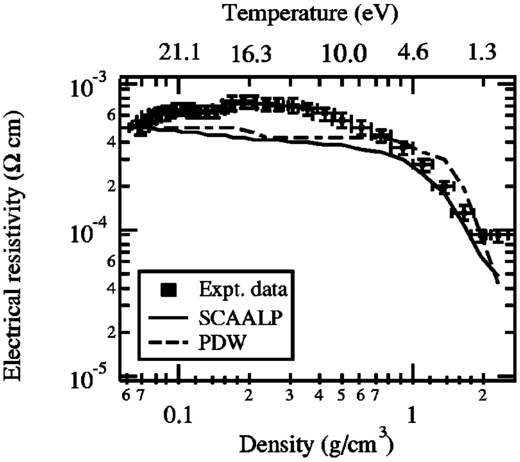

FIG. 3. Electrical resistivity of aluminum as a function of density. SCAALP and Perrot and Dharma-wardana (PDW) [30] calculations are compared to experimental data [4]. Temperature is scaled on the upper axis to show the conditions of the aluminum for these measurements.

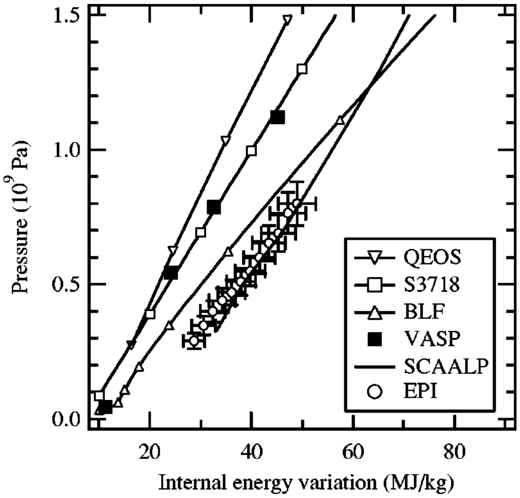

FIG. 4. Pressure of aluminum at a density of 0.1 $\mathrm{g\,cm^{-3}}$ as a function of internal energy variation. Theoretical results from five EOS models are compared to experimental data [9].

the double shoulder corresponds to ionization of L and K shells, respectively. We have checked that the Hugoniot curve tends to the classical limit equal to four times solid density at very high pressure. The cause of these shoulders is well known [38]. They correspond to the competition between the release of energy stocked as internal energy within the shell and the pressure of free electrons. When ionization begins, the energy of the shock is used mainly to depopulate the relevant shells and the material is very compressive. However, the pressure of free electrons in increasing number finally dominates again and the material becomes more difficult to compress.

In Fig. 3 we compare the electronic electrical resistivity calculated by SCAALP in the conditions of the experiment performed by Benage *et al.* [4]. This experiment is very interesting because the thermodynamic path inside the diagram density temperature starts in the supposedly well-characterized plasma phase, i.e., high temperature and low density, crosses the entire unknown interpolated region, and ends in another well-determined liquid-metal phase, i.e., low temperature and nearly solid density. SCAALP predictions are very good at low and high temperature, and the general tendency of the experimental curve is well reproduced. The same trend is found by Perrot and Dharma-wardana (PDW) [30], though the disagreement at low temperature with experimental data is more pronounced. However, neither SCAALP nor PDW can describe the finer structure around 0.2 $\mathrm{g\,cm^{-3}}$. This is quite surprising because this part is *a priori* not the most difficult one to describe, from a theoretical point of view [39].

The Hugoniot curve and the experiment of Benage *et al.* [4] were done by varying both temperature and density. A breakthrough in the field was made recently by the EPI group, who performed isochore measurements of pressure, internal energy variation, and electrical resistivity of an aluminum plasma at 0.1 $\mathrm{g\,cm^{-3}}$ in the warm dense matter regime [8,9]. The originality of the work consists of recording two equation of state quantities and one transport coefficient simultaneously. This major advance constitutes a stringent experimental constraint for any model designed to describe strongly coupled plasmas because the warm dense regime is the key point for testing the consistency between liquid metal and hot plasma treatments. As for equation of state, we see in Fig. 4 that SCAALP results agree well with experimental values. In the EPI regime, QEOS is not very accurate but this fact was already known. The most surprising result is the discrepancy between quantum molecular dynamics (QMD) calculations and EPI data. In fact, in the regime of partially ionized plasmas, the equation of state predictions obtained from QMD are as accurate as the results from the interpolated Sesame tables. As for electrical resistivity, we see in Fig. 5 that the agreement of SCAALP with the experiment is excellent, either concerning the EPI measurements or the exploded wire measurements [2,3]. This is good news, with regard to the simplicity of our approach based on the Ziman formula, which is known to be too crude in nearly neutral

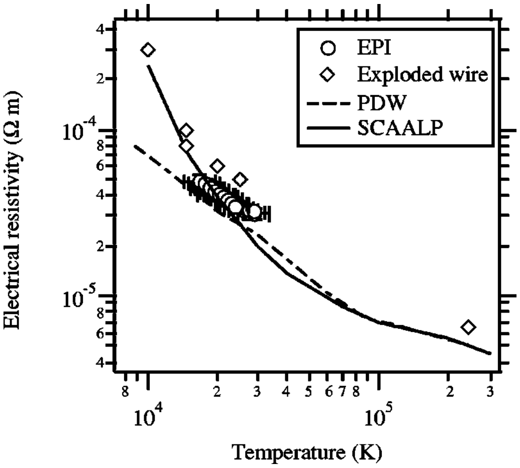

FIG. 5. Electrical resistivities of aluminum at 0.1 $\mathrm{g\,cm^{-3}}$ calculated by SCAALP and by Perrot and Dharma-wardana (PDW) [30] are compared to experimental data [2–4,8].

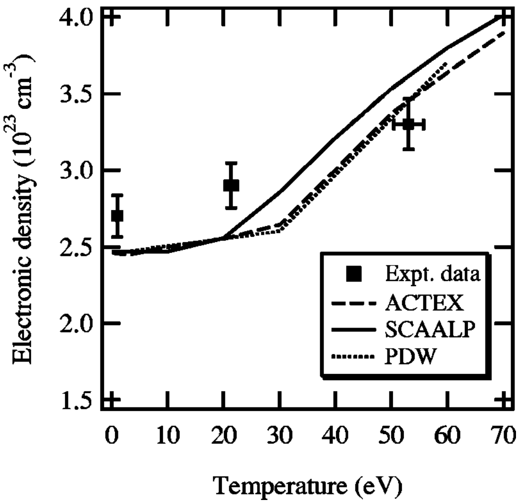

FIG. 6. Density-temperature phase diagram along with results of the x-ray scattering measurements and simulation using the ACTEX model [43,44], the Perrot and Dharma-wardana model (PDW) [45], and the SCAALP model.

media [40,41]. As for the approach of Perrot and Dharma-wardana, SCAALP and PDW calculations are very closed, except at lower temperature where PDW calculations differ from the resistivity measured by the exploded wire technique.

We end this section by comparing SCAALP electronic density estimates to measurements for a beryllium plasma at solid density [42] in Fig. 6. From these experiments, the ratio of delocalized to localized electronic densities can be obtained from the analysis of x-ray Thomson scattering. At low temperature, the agreement between SCAALP, ACTEX [43,44], the Perrot and Dharma-wardana's approach [45], and experimental results is good. In these conditions, SCAALP predicts a density of states perturbed by resonances due to quasibound states. Predictions of all these first-principles but different models are similar and close to experimental results.

IV. CONCLUSIONS AND PERSPECTIVES

In this paper, we have presented an *ab initio* and computationable model to describe the thermodynamic and transport properties of dense plasmas. The electronic and ionic structures are determined solving mean-field equations, which are deduced from a variational approach based on the Gibbs-Bogolyubov inequality. This ensures a self-consistent treatment between the electronic structure, found solving an effective one-electron Schrödinger equation using the density functional theory within the framework of the local density approximation, and the ionic distribution, found from the Gibbs-Bogolyubov inequality employing OCP or HS as reference system. Confrontation between theoretical and experimental results available in the literature of dense plasmas, i.e., cold curve, Hugoniot curve, ionization, electrical resistivity, and calorific properties, shows that SCAALP predictions are good.

We could also proceed from spherical to nonspherical symmetry, and consider the treatment of molecules or clusters. Derivation of equations is tedious but relatively simple to obtain. It is just a matter of algebra, once settled the overall theoretical framework. The use of a ionic reference system could also be bypassed, connecting directly the pair distribution to the effective ion-ion potential using Monte Carlo or molecular dynamics simulations. These techniques are very powerful and many interesting results have been obtained with them. However, they are not black-box algorithms and we think it is unrealistic to try to implement them inside the convergence process. However, they could be of great utility once achieved the overall convergence of the SCAALP process, i.e., as postprocessors for some particular diagnostics (microfield distribution, nearest-neighbor distribution, dynamic structure factor, transport coefficients).

ACKNOWLEDGMENTS

We thank D. Gogny, S. Kiyokawa, and R. M. More for helpful discussions, P. Renaudin for extensive and careful use of SCAALP, figures of this paper, as well as for his constructive remarks, comments, and constant support at each development phase of this work, and A. Greene for the careful reading of the document.

APPENDIX A: STATISTICAL AVERAGE USING ONE-ELECTRON HAMILTONIAN

In this appendix, we are going to calculate the thermal average $\langle \hat{H}_e \rangle_{e0}$ of the electronic Hamiltonian part $\hat{H}_e$ of the total Hamiltonian of the system given in Eq. (3), using the eigenstates of the one-electron Hamiltonian $\hat{H}_{e0}$ [19,46,20]. We recall that

$$\langle \{ \cdots \} \rangle_{e0} = \frac{\mathrm{Tr}_e [e^{-\beta(\hat{H}_{e0} - \mu_e \hat{N}_e)} \{ \cdots \}]}{e^{-\beta \Omega_{e0}}},$$

$$e^{-\beta \Omega_{e0}} = \mathrm{Tr}_e [e^{-\beta(\hat{H}_{e0} - \mu_e \hat{N}_e)}], \tag{A1}$$

where $\hat{N}_e$ is the electron number operator, β the inverse temperature, and μ_e the electronic chemical potential. Starting from Eq. (3), it is easy to find a more convenient expression of $\hat{H}_e$ using second-quantification operator algebra,

$$\hat{H}_e = \int \hat{\Psi}^\dagger(\mathbf{r}) h(\mathbf{r}, \{\mathbf{R}\}) \hat{\Psi}(\mathbf{r}) d\mathbf{r},$$

$$+ \frac{1}{2} \int \int \hat{\Psi}^\dagger(\mathbf{r}) \hat{\Psi}^\dagger(\mathbf{r}') \frac{e^2}{|\mathbf{r} - \mathbf{r}'|} \hat{\Psi}(\mathbf{r}') \hat{\Psi}(\mathbf{r}) d\mathbf{r} d\mathbf{r}', \tag{A2}$$

with

$$h(\mathbf{r}, \{\mathbf{R}\}) = -\frac{\hbar^2 \nabla^2}{2m} - \sum_j \frac{Z_I e^2}{|\mathbf{r} - \mathbf{R}_j|}, \tag{A3}$$

and where the electronic field operator $\hat{\Psi}(\mathbf{r})$, which is a function of electron and nuclei positions, can be written as

$$\hat{\Psi}(\mathbf{r})=\sum_j \sum_n \varphi_n(\mathbf{r}-\mathbf{R}_j)\hat{\mathbf{a}}_{jn}. \tag{A4}$$

$\hat{\mathbf{a}}_{jn}$ is the annihilation operator acting on an electron with a quantum state n in the jth ion. These operators verify the following anticommutation relations:

$$\{\hat{\mathbf{a}}^\dagger_{in},\hat{\mathbf{a}}_{jm}\}=\delta_{ij}\delta_{nm}, \tag{A5}$$

$$\{\hat{\mathbf{a}}^\dagger_{in},\hat{\mathbf{a}}^\dagger_{jm}\}=\{\hat{\mathbf{a}}_{in},\hat{\mathbf{a}}_{jm}\}=0. \tag{A6}$$

Equation (A5) means that two electrons are independent of each other when one electron is in an ion and the other is in another one. Thus, $\hat{H}_e$ can be rewritten as

$$\begin{aligned}\hat{H}_e={}&\sum_{i,j}\sum_{n,m}\int \varphi_n^*(\mathbf{r}-\mathbf{R}_i)h(\mathbf{r},\{\mathbf{R}\})\varphi_m(\mathbf{r}-\mathbf{R}_i)d\mathbf{r}\hat{\mathbf{a}}^\dagger_{in}\hat{\mathbf{a}}_{jm}\\&+\frac{1}{2}\sum_{i,j,k,l}\sum_{n_1,n_2,n_3,n_4}\int\int \varphi_{n_1}^*(\mathbf{r}-\mathbf{R}_i)\varphi_{n_2}^*(\mathbf{r}'-\mathbf{R}_j)\\&\times\frac{e^2}{|\mathbf{r}-\mathbf{r}'|}\varphi_{n_3}(\mathbf{r}'-\mathbf{R}_k)\varphi_{n_4}(\mathbf{r}-\mathbf{R}_l)d\mathbf{r}d\mathbf{r}'\hat{\mathbf{a}}^\dagger_{in_1}\hat{\mathbf{a}}^\dagger_{jn_2}\hat{\mathbf{a}}_{kn_3}\hat{\mathbf{a}}_{ln_4}\end{aligned} \tag{A7}$$

Let us introduce the unperturbed Hamiltonian operator $\hat{H}_{e0}$:

$$\hat{H}_{e0}=\sum_j\sum_n \varepsilon_n\hat{\mathbf{a}}^\dagger_{jn}\hat{\mathbf{a}}_{jn}. \tag{A8}$$

Since we assume that neutral "atoms" of the whole unperturbed Hamiltonian do not interact with each other, the one-electron energy ε_n logically does not depend on label j. The one-electron wave function $\varphi_n(\mathbf{r})$ and energy ε_n are solutions of a Schrödinger equation with a central symmetric effective potential $v_{eff}(\mathbf{r})$:

$$\left[-\frac{\hbar^2\nabla^2}{2m}+v_{eff}(\mathbf{r})\right]\varphi_n(\mathbf{r})=\varepsilon_n\varphi_n(\mathbf{r}). \tag{A9}$$

$v_{eff}(\mathbf{r})$, still unknown, must be determined self-consistently as will be seen below. The thermal average of the Hamiltonian $\hat{H}_e$ can be performed using the eigenstates of $\hat{H}_{e0}$. Derivation is standard but quite tedious. It can be highly simplified if we use the thermal average of a product of two operators:

$$\langle\hat{\mathbf{a}}^\dagger_{in}\hat{\mathbf{a}}_{jm}\rangle=f_n\delta_{ij}\delta_{nm}, \tag{A10}$$

where f_n is given by

$$f_n=\frac{1}{\exp([\beta(\varepsilon_n-\mu_e)]+1)}, \tag{A11}$$

and the Wick's theorem to reduce the four operator expectation values,

$$\begin{aligned}\langle\hat{\mathbf{a}}^\dagger_{in_1}\hat{\mathbf{a}}^\dagger_{jn_2}\hat{\mathbf{a}}_{kn_3}\hat{\mathbf{a}}_{\mathrm{l}n_4}\rangle={}&-\delta_{ik}\delta_{n_1n_3}\delta_{jl}\delta_{n_2n_4}f_{n_1}f_{n_2}\\&+\delta_{il}\delta_{n_1n_4}\delta_{jk}\delta_{n_2n_3}f_{n_1}f_{n_2}.\end{aligned} \tag{A12}$$

The thermal average of the Hamiltonian $\hat{H}_e$ is then calculated as follows:

$$\begin{aligned}\langle\hat{H}_e\rangle_{e0}={}&\sum_i\sum_n\int\varphi_n^*(\mathbf{r}-\mathbf{R}_i)h(\mathbf{r},\{\mathbf{R}\})\varphi_n(\mathbf{r}-\mathbf{R}_i)d\mathbf{r}f_n\\&+\frac{1}{2}\sum_{i,j}\sum_{n_1,n_2}\int\int\varphi_{n_1}^*(\mathbf{r}-\mathbf{R}_i)\varphi_{n_2}^*(\mathbf{r}'-\mathbf{R}_j)\\&\times\frac{e^2}{|\mathbf{r}-\mathbf{r}'|}\varphi_{n_2}(\mathbf{r}'-\mathbf{R}_j)\varphi_{n_1}(\mathbf{r}-\mathbf{R}_i)d\mathbf{r}d\mathbf{r}'f_{n_1}f_{n_2}\\&-\frac{1}{2}\sum_{i,j}\sum_{n_1,n_2}\int\int\varphi_{n_1}^*(\mathbf{r}-\mathbf{R}_i)\varphi_{n_2}^*(\mathbf{r}'-\mathbf{R}_j)\\&\times\frac{e^2}{|\mathbf{r}-\mathbf{r}'|}\varphi_{n_1}(\mathbf{r}'-\mathbf{R}_i)\varphi_{n_2}(\mathbf{r}-\mathbf{R}_j)d\mathbf{r}d\mathbf{r}'f_{n_1}f_{n_2},\end{aligned} \tag{A13}$$

or, by using Eq. (A3),

$$\begin{aligned}\langle\hat{H}_e\rangle_{e0}={}&\sum_i\sum_n\int\varphi_n^*(\mathbf{r}-\mathbf{R}_i)\left[-\frac{\hbar^2\nabla^2}{2m}-\sum_j\frac{Z_Ie^2}{|\mathbf{r}-\mathbf{R}_j|}\right]\\&\times\varphi_n(\mathbf{r}-\mathbf{R}_i)d\mathbf{r}f_n+\frac{1}{2}\sum_{i,j}\sum_{n_1,n_2}\int\int\varphi_{n_1}^*(\mathbf{r}-\mathbf{R}_i)\\&\times\varphi_{n_2}^*(\mathbf{r}'-\mathbf{R}_j)\frac{e^2}{|\mathbf{r}-\mathbf{r}'|}\varphi_{n_2}(\mathbf{r}'-\mathbf{R}_j)\varphi_{n_1}(\mathbf{r}-\mathbf{R}_i)\\&\times d\mathbf{r}d\mathbf{r}'f_{n_1}f_{n_2}-\frac{1}{2}\sum_{i,j}\sum_{n_1,n_2}\int\int\varphi_{n_1}^*(\mathbf{r}-\mathbf{R}_i)\\&\times\varphi_{n_2}^*(\mathbf{r}'-\mathbf{R}_j)\frac{e^2}{|\mathbf{r}-\mathbf{r}'|}\varphi_{n_1}(\mathbf{r}'-\mathbf{R}_i)\varphi_{n_2}(\mathbf{r}-\mathbf{R}_j)\\&\times d\mathbf{r}d\mathbf{r}'f_{n_1}f_{n_2}.\end{aligned} \tag{A14}$$

We simply find a finite-temperature Hartree-Fock expression for $\langle\hat{H}_e\rangle_{e0}$, with additional terms arising from the various nuclei of the system. As $\boldsymbol{\nabla}$ acts only on electron coordinates, we define K_e as the electron kinetic energy (calculated at $\mathbf{R}_i=0$):

$$K_e=-\int\sum_n f_n\varphi_n^*(\mathbf{r})\frac{\hbar^2\nabla^2}{2m}\varphi_n(\mathbf{r})d\mathbf{r}. \tag{A15}$$

It is thus quite natural to introduce

$$\rho_e(\mathbf{r})=\sum_n f_n\varphi_n^*(\mathbf{r})\varphi_n(\mathbf{r}). \tag{A16}$$

Since the $\varphi_n(\mathbf{r})$ are the same for all neutral atoms,

$$
\begin{aligned}
\langle \hat{H}_e \rangle_{e0} = {} & N_I K_e - \sum_{i,j} Z_I e^2 \int \frac{\rho_e(\mathbf{r}-\mathbf{R}_i)}{|\mathbf{r}-\mathbf{R}_j|} d\mathbf{r} \\
& + \frac{e^2}{2} \sum_{i,j} \int \int \frac{\rho_e(\mathbf{r}-\mathbf{R}_i)\rho_e(\mathbf{r}'-\mathbf{R}_j)}{|\mathbf{r}-\mathbf{r}'|} d\mathbf{r} d\mathbf{r}' \\
& - \frac{1}{2} \sum_{i} \sum_{n_1,n_2} \int \int \varphi_{n_1^*}(\mathbf{r}-\mathbf{R}_i) \varphi_{n_2^*}(\mathbf{r}'-\mathbf{R}_i) \\
& \times \frac{e^2}{|\mathbf{r}-\mathbf{r}'|} \varphi_{n_1}(\mathbf{r}'-\mathbf{R}_i) \varphi_{n_2}(\mathbf{r}-\mathbf{R}_i) d\mathbf{r} d\mathbf{r}' f_{n_1} f_{n_2} \\
& - \frac{1}{2} \sum_{i \neq j} \sum_{n_1,n_2} \int \int \varphi_{n_1^*}(\mathbf{r}-\mathbf{R}_i) \varphi_{n_2^*}(\mathbf{r}'-\mathbf{R}_j) \\
& \times \frac{e^2}{|\mathbf{r}-\mathbf{r}'|} \varphi_{n_1}(\mathbf{r}'-\mathbf{R}_i) \varphi_{n_2}(\mathbf{r}-\mathbf{R}_j) d\mathbf{r} d\mathbf{r}' f_{n_1} f_{n_2}.
\end{aligned}
\tag{A17}
$$

Using $\tilde{\mathbf{r}} = \mathbf{r} - \mathbf{R}_i$, $\tilde{\mathbf{r}}' = \mathbf{r}' - \mathbf{R}_i$, and $\mathbf{R}_{ji} = \mathbf{R}_j - \mathbf{R}_i$,

$$
\begin{aligned}
\langle \hat{H}_e \rangle_{e0} = {} & N_I K_e - \sum_{i,j} Z_I e^2 \int \frac{\rho_e(\mathbf{r}-\mathbf{R}_i)}{|\mathbf{r}-\mathbf{R}_j|} d\mathbf{r} \\
& + \frac{e^2}{2} \sum_{i,j} \int \int \frac{\rho_e(\mathbf{r}-\mathbf{R}_i)\rho_e(\mathbf{r}'-\mathbf{R}_j)}{|\mathbf{r}-\mathbf{r}'|} d\mathbf{r} d\mathbf{r}' \\
& - \frac{1}{2} \sum_{i} \sum_{n_1,n_2} \int \int \varphi_{n_1^*}(\tilde{\mathbf{r}}) \varphi_{n_2^*}(\tilde{\mathbf{r}}') \frac{e^2}{|\tilde{\mathbf{r}}-\tilde{\mathbf{r}}'|} \\
& \times \varphi_{n_1}(\tilde{\mathbf{r}}') \varphi_{n_2}(\tilde{\mathbf{r}}) d\tilde{\mathbf{r}} d\tilde{\mathbf{r}}' f_{n_1} f_{n_2} \\
& - \frac{1}{2} \sum_{i \neq j} \sum_{n_1,n_2} \int \int \varphi_{n_1^*}(\tilde{\mathbf{r}}) \varphi_{n_2^*}(\tilde{\mathbf{r}}'-\mathbf{R}_{ji}) \\
& \times \frac{e^2}{|\tilde{\mathbf{r}}-\tilde{\mathbf{r}}'|} \varphi_{n_1}(\tilde{\mathbf{r}}') \varphi_{n_2}(\tilde{\mathbf{r}}-\mathbf{R}_{ji}) d\tilde{\mathbf{r}} d\tilde{\mathbf{r}}' f_{n_1} f_{n_2}.
\end{aligned}
\tag{A18}
$$

The fourth and fifth terms on the right-hand side of the above equation are the exchange energy $E_X(\mathbf{R}_{ji}=0)$ and $E_X(\mathbf{R}_{ji} \neq 0)$, respectively. $\langle \hat{H}_e \rangle$ can be put into a more compact form,

$$
\begin{aligned}
\langle \hat{H}_e \rangle_{e0} = {} & N_I K_e + N_I E_X(0) + \sum_{i \neq j} E_X(\mathbf{R}_{ji}) \\
& - \sum_{i} Z_I e^2 \int \frac{\rho_e(\tilde{\mathbf{r}})}{|\tilde{\mathbf{r}}|} d\tilde{\mathbf{r}} \\
& + \frac{e^2}{2} \sum_{i} \int \int \frac{\rho_e(\tilde{\mathbf{r}})\rho_e(\tilde{\mathbf{r}}')}{|\tilde{\mathbf{r}}-\tilde{\mathbf{r}}'|} d\tilde{\mathbf{r}} d\tilde{\mathbf{r}}' \\
& - \sum_{i \neq j} Z_I e^2 \int \frac{\rho_e(\mathbf{r}-\mathbf{R}_i)}{|\mathbf{r}-\mathbf{R}_j|} d\mathbf{r} \\
& + \frac{e^2}{2} \sum_{i \neq j} \int \int \frac{\rho_e(\mathbf{r}-\mathbf{R}_i)\rho_e(\mathbf{r}'-\mathbf{R}_j)}{|\mathbf{r}-\mathbf{r}'|} d\mathbf{r} d\mathbf{r}'
\end{aligned}
\tag{A19}
$$

The fourth and fifth terms on the right-hand side of the above equation do not depend on label i:

$$
\begin{aligned}
\langle \hat{H}_e \rangle_{e0} = {} & N_I \Bigg[K_e + E_X(0) - Z_I e^2 \int \frac{\rho_e(\tilde{\mathbf{r}})}{|\tilde{\mathbf{r}}|} d\tilde{\mathbf{r}} \\
& + \frac{e^2}{2} \int \int \frac{\rho_e(\tilde{\mathbf{r}})\rho_e(\tilde{\mathbf{r}}')}{|\tilde{\mathbf{r}}-\tilde{\mathbf{r}}'|} d\tilde{\mathbf{r}} d\tilde{\mathbf{r}}' \Bigg] \\
& + \frac{1}{2} \sum_{i \neq j} \Bigg[2E_X(\mathbf{R}_{ji}) - 2 Z_I e^2 \int \frac{\rho_e(\mathbf{r}-\mathbf{R}_i)}{|\mathbf{r}-\mathbf{R}_j|} d\mathbf{r} \\
& + e^2 \int \int \frac{\rho_e(\mathbf{r}-\mathbf{R}_i)\rho_e(\mathbf{r}'-\mathbf{R}_j)}{|\mathbf{r}-\mathbf{r}'|} d\mathbf{r} d\mathbf{r}' \Bigg].
\end{aligned}
\tag{A20}
$$

The part of the above equation that depends on nucleus positions can be rewritten as (with $\tilde{\mathbf{r}}' = \mathbf{r}' - \mathbf{R}_j$):

$$
\begin{aligned}
& 2E_X(\mathbf{R}_{ji}) - \frac{Z_I^2 e^2}{|\mathbf{R}_{ji}|} + \frac{Z_I^2 e^2}{|\mathbf{R}_{ji}|} - 2 Z_I e^2 \int \frac{\rho_e(\tilde{\mathbf{r}})}{|\tilde{\mathbf{r}}-\mathbf{R}_{ji}|} d\tilde{\mathbf{r}} \\
& \quad + e^2 \int \int \frac{\rho_e(\mathbf{r}-\mathbf{R}_i)\rho_e(\mathbf{r}'-\mathbf{R}_j)}{|\mathbf{r}-\mathbf{r}'|} d\mathbf{r} d\mathbf{r}' \\
& \quad = 2E_X(\mathbf{R}_{ji}) - \frac{Z_I^2 e^2}{|\mathbf{R}_{ji}|} - Z_I \left[-\frac{Z_I e^2}{|\mathbf{R}_{ji}|} + e^2 \int \frac{\rho_e(\tilde{\mathbf{r}})}{|\mathbf{R}_{ji}-\tilde{\mathbf{r}}|} d\tilde{\mathbf{r}} \right] \\
& \qquad - Z_I e^2 \int \frac{\rho_e(\tilde{\mathbf{r}})}{|\tilde{\mathbf{r}}-\mathbf{R}_{ji}|} d\tilde{\mathbf{r}} + e^2 \int \int \frac{\rho_e(\tilde{\mathbf{r}})\rho_e(\tilde{\mathbf{r}}')}{|\tilde{\mathbf{r}}-\mathbf{R}_{ji}-\tilde{\mathbf{r}}'|} d\tilde{\mathbf{r}} d\tilde{\mathbf{r}}' \\
& \quad = 2E_X(\mathbf{R}_{ji}) - \frac{Z_I^2 e^2}{|\mathbf{R}_{ji}|} - Z_I v_{at}(\mathbf{R}_{ji}) + \int \rho_e(\tilde{\mathbf{r}}) v_{at}(\tilde{\mathbf{r}}-\mathbf{R}_{ji}),
\end{aligned}
\tag{A21}
$$

where

$$
v_{at}(\mathbf{r}) = -\frac{Z_I e^2}{|\mathbf{r}|} + e^2 \int \frac{\rho_e(\mathbf{r}')}{|\mathbf{r}-\mathbf{r}'|}. \tag{A22}
$$

Finally, the thermal average of the Hamiltonian $\hat{H}_e$ verifies

$$
\begin{aligned}
\langle \hat{H}_e \rangle_{e0} = {} & N_I \Bigg[K_e + E_X(0) - Z_I e^2 \int \frac{\rho_e(\tilde{\mathbf{r}})}{|\tilde{\mathbf{r}}|} d\tilde{\mathbf{r}} \\
& + \frac{e^2}{2} \int \int \frac{\rho_e(\tilde{\mathbf{r}})\rho_e(\tilde{\mathbf{r}}')}{|\tilde{\mathbf{r}}-\tilde{\mathbf{r}}'|} d\tilde{\mathbf{r}} d\tilde{\mathbf{r}}' \Bigg] \\
& + \frac{1}{2} \sum_{i \neq j} \left[-\frac{Z_I^2 e^2}{|\mathbf{R}_{ji}|} + \Phi(\mathbf{R}_{ji}) \right],
\end{aligned}
\tag{A23}
$$

where

$$
\Phi(\mathbf{R}) = 2E_X(\mathbf{R}) - Z_I v_{at}(\mathbf{R}) + \int \rho_e(\tilde{\mathbf{r}}) v_{at}(\tilde{\mathbf{r}}-\mathbf{R}) d\tilde{\mathbf{r}}. \tag{A24}
$$

The thermal average $\langle \hat{H}_{e0} \rangle_{e0}$ of the one-electron Hamiltonian $\hat{H}_{e0}$ reads

$$\langle \hat{H}_{e0}\rangle_{e0}=N_I\sum_n \varepsilon_n f_n . \tag{A25}$$

Furthermore, using the second identity of Eq. (A1),

$$\Omega_{e0}=-\frac{N_I}{\beta}\sum_n \ln[1+e^{-\beta(\varepsilon_n-\mu_e)}]. \tag{A26}$$

Indeed, multiplying Eq. (A9) by $f_n\varphi_n^*(\mathbf{r})$ on the left, integrating over $\mathbf{r}$, and using Eq. (A16), the kinetic energy K_e given by Eq. (A15) can also be expressed as

$$K_e=\sum_n \varepsilon_n f_n-\int v_{eff}(\mathbf{r})\rho_e(\mathbf{r})d\mathbf{r}. \tag{A27}$$

Finally, combining Eqs. (A23), (A25), and (A27) leads naturally to the working formula for the thermal average $\langle \hat{H}_e-\hat{H}_{e0}\rangle_{e0}$, i.e.,

$$\begin{aligned}\langle \hat{H}_e-\hat{H}_{e0}\rangle_{e0}=&N_I\left[E_X(0)-\frac{e^2}{2}\int\int\frac{\rho_e(\tilde{\mathbf{r}})\rho_e(\tilde{\mathbf{r}}')}{|\tilde{\mathbf{r}}-\tilde{\mathbf{r}}'|}d\tilde{\mathbf{r}}d\tilde{\mathbf{r}}'\right]\\&+N_I\left[\int\rho_e(\tilde{\mathbf{r}})v_{at}(\tilde{\mathbf{r}})d\tilde{\mathbf{r}}-\int\rho_e(\tilde{\mathbf{r}})v_{eff}(\tilde{\mathbf{r}})d\tilde{\mathbf{r}}\right]\\&+\frac{1}{2}\sum_{i\neq j}\left[-\frac{Z_I^2e^2}{|\mathbf{R}_{ji}|}+\Phi(\mathbf{R}_{ji})\right],\end{aligned} \tag{A28}$$

which is simply Eq. (15).

APPENDIX B: STATISTICAL AVERAGE USING IONIC REFERENCE SYSTEM

In this appendix, we are going to derive Eq. (26) starting from Eq. (22). The proof is in fact a strict application of the GBI to simple fluid interacting through pair potential [22,23]. We want just to focus on some tricky terms arising due to the presence of a neutralizing background in the reference system. So, let us start from Eq. (22), which gives the excess free energy of a system of N_I particles interacting through a two-body potential $\Phi(\mathbf{R})$,

$$\mathrm{tr}_I\left[\exp\left(-\frac{\beta}{2}\sum_{i\neq j}\Phi(\mathbf{R}_{ji})\right)\right]=e^{-\beta F_\Phi^{ex}}, \tag{B1}$$

where

$$\mathrm{tr}_I\{\cdots\}=\int\frac{d^{N_I}\mathbf{R}}{V^{N_I}}\{\cdots\}. \tag{B2}$$

Let us suppose that we have a reference system of N_I particles interacting via a two-body potential $\Phi_{ref}(\lambda,\mathbf{R_i},\mathbf{R_j})$, for which the excess free energy $F_{ref}^{ex}(\lambda)$, the excess internal energy $U_{ref}^{ex}(\lambda)$, and the pair distribution $g_{ref}(\lambda,\mathbf{R_i},\mathbf{R_j})$ are known. Note that we do not implicitly assume that the interaction depends only on the relative distance between particles. We can thus insert in Eq. (B1) $\pm\Phi_{ref}(\lambda,\mathbf{R_i},\mathbf{R_j})$ near $\Phi(\mathbf{R}_{ji})$. Then, using

$$\begin{aligned}\langle\{\cdots\}\rangle_\lambda=&\frac{\mathrm{Tr}_e\left[\exp\left(-\dfrac{\beta}{2}\sum_{i\neq j}\Phi_{ref}(\lambda,\mathbf{R_i},\mathbf{R_j})\{\cdots\}\right)\right]}{e^{-\beta F_{ref}^{ex}(\lambda)}},\\ e^{-\beta F_{ref}^{ex}(\lambda)}=&\mathrm{tr}_I\left[\exp\left(-\frac{\beta}{2}\sum_{i\neq j}\Phi_{ref}(\lambda,\mathbf{R_i},\mathbf{R_j})\right)\right],\end{aligned} \tag{B3}$$

and the well-known property

$$\begin{aligned}&\left\langle\exp\left(-\frac{\beta}{2}\sum_{i\neq j}[\Phi(\mathbf{R}_{ij})-\Phi_{ref}(\lambda,\mathbf{R_i},\mathbf{R_j})]\right)\right\rangle_\lambda\\&\quad\geqslant\exp\left(-\left\langle\frac{\beta}{2}\sum_{i\neq j}[\Phi(\mathbf{R}_{ij})-\Phi_{ref}(\lambda,\mathbf{R_i},\mathbf{R_j})]\right\rangle_\lambda\right),\end{aligned} \tag{B4}$$

we have

$$F_\Phi^{ex}\leqslant F_{ref}^{ex}(\lambda)+\left\langle\frac{1}{2}\sum_{i\neq j}[\Phi(\mathbf{R}_{ij})-\Phi_{ref}(\lambda,\mathbf{R_i},\mathbf{R_j})]\right\rangle_\lambda . \tag{B5}$$

Since

$$U_{ref}^{ex}(\lambda)=\left\langle\frac{1}{2}\sum_{i\neq j}\Phi_{ref}(\lambda,\mathbf{R_i},\mathbf{R_j})\right\rangle_\lambda , \tag{B6}$$

we are left with

$$F_\Phi^{ex}\leqslant F_{ref}^{ex}(\lambda)-U_{ref}^{ex}(\lambda)+\left\langle\frac{1}{2}\sum_{i\neq j}[\Phi(\mathbf{R}_{ij})]\right\rangle_\lambda . \tag{B7}$$

Now, let us introduce the two-particle density $\delta^{(2)}(\mathbf{R},\mathbf{R}')$,

$$\delta^{(2)}(\mathbf{R},\mathbf{R}')=\sum_{i\neq j}\delta(|\mathbf{R}-\mathbf{R}_i|)\,\delta(|\mathbf{R}'-\mathbf{R}_j|), \tag{B8}$$

then

$$\left\langle\frac{1}{2}\sum_{i\neq j}[\Phi(\mathbf{R}_{ij})]\right\rangle_\lambda=\frac{1}{2}\int d\mathbf{R}d\mathbf{R}'\,\Phi(\mathbf{R}-\mathbf{R}')\langle\delta^{(2)}(\mathbf{R},\mathbf{R}')\rangle_\lambda \tag{B9}$$

or

$$\left\langle\frac{1}{2}\sum_{i\neq j}[\Phi(\mathbf{R}_{ij})]\right\rangle_\lambda=\frac{\rho_I^2}{2}\int d\mathbf{R}d\mathbf{R}'\,\Phi(\mathbf{R}-\mathbf{R}')g_{ref}(\lambda,\mathbf{R},\mathbf{R}') \tag{B10}$$

using the definition of the $g_{ref}(\lambda,\mathbf{R},\mathbf{R}')$, namely,

$$\rho_I^2 g_{ref}(\lambda,\mathbf{R},\mathbf{R}')=\langle\delta^{(2)}(\mathbf{R},\mathbf{R}')\rangle_\lambda . \tag{B11}$$

As a consequence,

$$\begin{aligned}F_\Phi^{ex}\leqslant&F_{ref}^{ex}(\lambda)-U_{ref}^{ex}(\lambda)+\frac{\rho_I^2}{2}\int d\mathbf{R}d\mathbf{R}'\\&\times\Phi(\mathbf{R}-\mathbf{R}')g_{ref}(\lambda,\mathbf{R},\mathbf{R}').\end{aligned} \tag{B12}$$

The right-hand side is an exact result. Our main approximation concerns the choice of the reference system. Since our original system is isotropic and homogenous, i.e., Φ depends only on the relative distance between particles, it is reasonable to choose a reference system with the same property. In that case,

$$g_{ref}(\lambda,\mathbf{R},\mathbf{R}')=g_{ref}(\lambda,\mathbf{R}-\mathbf{R}'), \tag{B13}$$

and we find Eq. (26),

$$F_{\Phi}^{ex}\leqslant F_{ref}^{ex}(\lambda)-U_{ref}^{ex}(\lambda)+\frac{N_I\rho_I}{2}\int d\mathbf{R}\Phi(\mathbf{R})g_{ref}(\lambda,\mathbf{R}). \tag{B14}$$

When no background is included in the reference system, for instance HS system, then

$$U_{ref}^{ex}(\lambda)=\frac{N_I\rho_I}{2}\int d\mathbf{R}\Phi(\lambda,\mathbf{R})g_{ref}(\lambda,\mathbf{R}). \tag{B15}$$

However, when in the reference system, the particles do not simply interact through $\Phi(\lambda,\mathbf{R})$, but with a homogeneous neutralizing background; one must also take into account the background-background interaction and some zero-energy reference too. This is a typical situation encountered with the YOCP system. In that case, one can show that

$$U_{ref}^{ex}(\Gamma,\kappa)=\frac{N_I\rho_I}{2}\int d\mathbf{R}\Phi(\Gamma,\kappa,\mathbf{R})h_{ref}(\Gamma,\kappa,\mathbf{R})-\frac{N_I}{\beta}\frac{\Gamma\kappa}{2}. \tag{B16}$$

We have thus two independent parameters Γ and κ. When YOCP reduces to OCP ($\kappa=0$), which is the only case considered in this work for the reasons explained above in the main text, we simply have the general form

$$U_{ref}^{ex}(\lambda)=\frac{N_I\rho_I}{2}\int d\mathbf{R}\Phi(\lambda,\mathbf{R})h_{ref}(\lambda,\mathbf{R}). \tag{B17}$$

In summary, we use Eq. (B15) without neutralizing background, but Eq. (B17) with neutralizing background. We give the general proof for both cases but only the HS system, and so Eq. (B15) is used for the numerical applications presented in this paper.

APPENDIX C: MINIMIZATION OF THE TOTAL FREE ENERGY OF THE SYSTEM

In this appendix, we are going to derive Eqs. (30) and (32) applying the GBI for the total free energy of the system F_{tot} given by Eqs. (28) and (25). The rule is strict but quite intuitive [46,20]. We are looking for the smallest upper bound F_{tot} of the true total free energy $F_{sys}=\Omega_{sys}/N_I+\mu_I+Z_I\mu_e$ of the system [19]. To do this, we are going to separate F_{tot} into two contributions, i.e., an electronic part

$$F_{tot}^{e}=\Omega_e+Z_I\mu_e, \tag{C1}$$

and an ionic part

$$F_{tot}^{I}=\frac{F_I^{id}+F_{ref}^{ex}(\lambda)-U_{ref}^{ex}(\lambda)}{N_I}+\frac{\rho_I}{2}\int d\mathbf{R}g_{ref}(\lambda,R)\Phi(\mathbf{R}). \tag{C2}$$

Let us consider first the minimization with respect to electronic density ρ_e,

$$\frac{\delta F_{tot}}{\delta\rho_e(\mathbf{r})}=0. \tag{C3}$$

As for F_{tot}^{I}, only the fourth term on the right-hand side of Eq. (C2) depends on $\rho_e(\mathbf{r})$ via $\Phi(\mathbf{R})$, so

$$\frac{\delta F_{tot}^{I}}{\delta\rho_e(\mathbf{r})}=\frac{\rho_I}{2}\int d\mathbf{R}g_{ref}(\lambda,R)\frac{\delta\Phi(\mathbf{R})}{\delta\rho_e(\mathbf{r})}. \tag{C4}$$

Using the definition of $\Phi(\mathbf{R})$, i.e., Eqs. (18) and (17), we have

$$\frac{\delta\Phi(\mathbf{R})}{\delta\rho_e(\mathbf{r})}=2\frac{\delta E_X(\mathbf{R})}{\delta\rho_e(\mathbf{r})}-Z_I\frac{\delta v_{at}(\mathbf{R})}{\delta\rho_e(\mathbf{r})}+v_{at}(\mathbf{r}-\mathbf{R})+\int\rho_e(\mathbf{r}')\frac{\delta v_{at}(\mathbf{r}'-\mathbf{R})}{\delta\rho_e(\mathbf{r})}d\mathbf{r}'. \tag{C5}$$

From Eq. (17), we know that

$$\frac{\delta v_{at}(\mathbf{r}')}{\delta\rho_e(\mathbf{r})}=\frac{e^2}{|\mathbf{r}-\mathbf{r}'|}. \tag{C6}$$

Yet, if we restrict ourselves to spherical symmetric problem, i.e.,

$$v_{at}(\mathbf{r}'-\mathbf{R})=v_{at}(|\mathbf{r}'-\mathbf{R}|)=v_{at}(|\mathbf{R}-\mathbf{r}'|)=v_{at}(\mathbf{R}-\mathbf{r}'), \tag{C7}$$

we arrive at

$$\frac{\delta\Phi(\mathbf{R})}{\delta\rho_e(\mathbf{r})}=2\frac{\delta E_X(\mathbf{R})}{\delta\rho_e(\mathbf{r})}-\frac{Z_Ie^2}{|\mathbf{r}-\mathbf{R}|}+v_{at}(\mathbf{r}-\mathbf{R})+\int\rho_e(\mathbf{r}')\frac{e^2}{|\mathbf{R}-\mathbf{r}'-\mathbf{r}|}d\mathbf{r}'. \tag{C8}$$

However, since

$$v_{at}(\mathbf{r}-\mathbf{R})=-\frac{Z_Ie^2}{|\mathbf{r}-\mathbf{R}|}+\int\rho_e(\mathbf{r}')\frac{e^2}{|\mathbf{R}-\mathbf{r}'-\mathbf{r}|}d\mathbf{r}', \tag{C9}$$

we get

$$\frac{1}{2}\frac{\delta\Phi(\mathbf{R})}{\delta\rho_e(\mathbf{r})}=\frac{\delta E_X(\mathbf{R})}{\delta\rho_e(\mathbf{r})}+v_{at}(\mathbf{r}-\mathbf{R}), \tag{C10}$$

which inserted into Eq. (C4) leads to

$$\frac{\delta F_{tot}^{I}}{\delta\rho_e(\mathbf{r})}=\rho_I\int d\mathbf{R}g_{ref}(\lambda,R)\left[\frac{\delta E_X(\mathbf{R})}{\delta\rho_e(\mathbf{r})}+v_{at}(\mathbf{r}-\mathbf{R})\right]. \tag{C11}$$

As for F^e_{tot} given by Eq. (C1),

$$\frac{\delta F^e_{tot}}{\delta\rho_e(\mathbf{r})}=\frac{\delta\Omega_e}{\delta\rho_e(\mathbf{r})}+Z_I\frac{\delta\mu_e}{\delta\rho_e(\mathbf{r})}. \tag{C12}$$

Using Eqs. (25) and (20),

$$\begin{aligned}\frac{\delta F^e_{tot}}{\delta\rho_e(\mathbf{r})}=&\sum_n f_n\frac{\delta(\varepsilon_n-\mu_e)}{\delta\rho_e(\mathbf{r})}+\frac{\delta E_X(\mathbf{0})}{\delta\rho_e(\mathbf{r})}-e^2\int\frac{\rho_e(\mathbf{r}')}{|\mathbf{r}-\mathbf{r}'|}d\mathbf{r}'\\&+Z_I\frac{\delta\mu_e}{\delta\rho_e(\mathbf{r})}+v_{at}(\mathbf{r})+\int\rho_e(\mathbf{r}')\frac{\delta v_{at}(\mathbf{r}')}{\delta\rho_e(\mathbf{r})}d\mathbf{r}'\\&-v_{eff}(\mathbf{r})-\int\rho_e(\mathbf{r}')\frac{\delta v_{eff}(\mathbf{r}')}{\delta\rho_e(\mathbf{r})}d\mathbf{r}'.\end{aligned} \tag{C13}$$

Using now Eq. (C6) and $\int\rho_e(\mathbf{r})d\mathbf{r}=\Sigma_n f_n=Z_I$,

$$\begin{aligned}\frac{\delta F^e_{tot}}{\delta\rho_e(\mathbf{r})}=&\sum_n f_n\frac{\delta\varepsilon_n}{\delta\rho_e(\mathbf{r})}+\frac{\delta E_X(\mathbf{0})}{\delta\rho_e(\mathbf{r})}+v_{at}(\mathbf{r})-v_{eff}(\mathbf{r})\\&-\int\rho_e(\mathbf{r}')\frac{\delta v_{eff}(\mathbf{r}')}{\delta\rho_e(\mathbf{r})}d\mathbf{r}'.\end{aligned} \tag{C14}$$

Yet, a straightforward application of first-order perturbation theory to Eq. (14) leads to

$$\frac{\delta\varepsilon_n}{\delta\rho_e(\mathbf{r})}=\int\rho_e(\mathbf{r}')\frac{\delta v_{eff}(\mathbf{r}')}{\delta\rho_e(\mathbf{r})}d\mathbf{r}', \tag{C15}$$

and

$$\frac{\delta F^e_{tot}}{\delta\rho_e(\mathbf{r})}=\frac{\delta E_X(\mathbf{0})}{\delta\rho_e(\mathbf{r})}+v_{at}(\mathbf{r})-v_{eff}(\mathbf{r}). \tag{C16}$$

Equation (C15) can also be obtained directly from Eq. (14) by noting that eigenfunctions $\varphi_n(\mathbf{r})$ are orthonormal. We adopt for this example the bra and ket Dirac notation, i.e., $\varphi_n(\mathbf{r})=\langle\mathbf{r}|n\rangle$, $\langle n|n'\rangle=\delta_{nn'}$. Let us multiply on the left Eq. (14) by $\langle n|$,

$$\langle n|-\frac{\hbar^2\nabla^2}{2m}+v_{eff}|n\rangle=\varepsilon_n, \tag{C17}$$

and differentiate with respect to $\rho_e(\mathbf{r})$. We get

$$\begin{aligned}\frac{\delta\varepsilon_n}{\delta\rho_e(\mathbf{r})}=&\frac{\delta\langle n|}{\delta\rho_e(\mathbf{r})}\left[-\frac{\hbar^2\nabla^2}{2m}+v_{eff}\right]|n\rangle\\&+\langle n|\frac{\delta\left[-\frac{\hbar^2\nabla^2}{2m}+v_{eff}\right]}{\delta\rho_e(\mathbf{r})}|n\rangle\\&+\langle n|\left[-\frac{\hbar^2\nabla^2}{2m}+v_{eff}\right]\frac{\delta|n\rangle}{\delta\rho_e(\mathbf{r})},\end{aligned} \tag{C18}$$

$$\begin{aligned}\frac{\delta\varepsilon_n}{\delta\rho_e(\mathbf{r})}=&\frac{\delta\langle n|}{\delta\rho_e(\mathbf{r})}|n\rangle\varepsilon_n+\langle n|\frac{\delta\left[-\frac{\hbar^2\nabla^2}{2m}+v_{eff}\right]}{\delta\rho_e(\mathbf{r})}|n\rangle\\&+\varepsilon_n\langle n|\frac{\delta|n}{\delta\rho_e(\mathbf{r})},\end{aligned} \tag{C19}$$

But, since $\langle n|n\rangle=1$,

$$\frac{\delta\langle n|}{\delta\rho_e(\mathbf{r})}|n\rangle=0, \tag{C20}$$

hence Eq. (C15). Finally, inserting Eqs. (C11) and (C16) into the minimum criterium (C3) gives

$$\begin{aligned}v_{eff}(\mathbf{r})=&v_{at}(\mathbf{r})+\frac{\delta E_X(0)}{\delta\rho_e(\mathbf{r})}+\rho_I\int\left[v_{at}(\mathbf{r}-\mathbf{R})\right.\\&\left.+\frac{\delta E_X(\mathbf{R})}{\delta\rho_e(\mathbf{r})}\right]g_{ref}(\lambda,\mathbf{R})d\mathbf{R},\end{aligned} \tag{C21}$$

which is result (32).

Let us now consider the minimization with respect to effective parameter λ,

$$\frac{\partial F_{tot}}{\partial\lambda}=0. \tag{C22}$$

Since F^e_{tot} is independent of λ, only F^I_{tot} matters. Using Eq. (C2), we have

$$\frac{\partial F^I_{tot}}{\partial\lambda}=\frac{1}{N_I}\left(\frac{\partial F^{ex}_{ref}}{\partial\lambda}-\frac{\partial U^{ex}_{ref}}{\partial\lambda}\right)+\frac{\rho_I}{2}\int d\mathbf{R}\frac{\partial g_{ref}(\lambda,R)}{\partial\lambda}\Phi_{ref}(\mathbf{R}). \tag{C23}$$

Using either Eq. (B15) or Eq. (B17) of precedent paragraph, we get

$$\begin{aligned}\frac{\partial U^{ex}_{ref}}{\partial\lambda}=&\frac{N_I\rho_I}{2}\int d\mathbf{R}\left[\frac{\partial\Phi_{ref}(\lambda,\mathbf{R})}{\partial\lambda}g_{ref}(\lambda,\mathbf{R})\right.\\&\left.+\Phi_{ref}(\lambda,\mathbf{R})\frac{\partial g_{ref}(\lambda,\mathbf{R})}{\partial\lambda}\right].\end{aligned} \tag{C24}$$

Differentiating with respect to λ the second equation of Eq. (B3), we get

$$\begin{aligned}\frac{\partial F^{ex}_{ref}}{\partial\lambda}e^{-\beta F^{ex}_{ref}(\lambda)}=&\mathrm{tr}_I\left[\frac{1}{2}\sum_{i\neq j}\frac{\partial\Phi_{ref}(\lambda,\mathbf{R_i},\mathbf{R_j})}{\partial\lambda}\right.\\&\left.\times\exp\left(-\frac{\beta}{2}\sum_{i\neq j}\Phi_{ref}(\lambda,\mathbf{R_i},\mathbf{R_j})\right)\right],\end{aligned} \tag{C25}$$

or

$$\frac{\partial F^{ex}_{ref}}{\partial\lambda}=\left\langle\frac{1}{2}\sum_{i\neq j}\frac{\partial\Phi_{ref}(\lambda,\mathbf{R_i},\mathbf{R_j})}{\partial\lambda}\right\rangle_\lambda, \tag{C26}$$

remembering the first equation of Eq. (B3). Since we assume the reference system to be homogenous and isotropic, we can follow the same reasoning of the last part of Appendix A to arrive at

$$\frac{\partial F^{ex}_{ref}}{\partial\lambda}=\frac{N_I\rho_I}{2}\int d\mathbf{R}\frac{\partial\Phi(\lambda,\mathbf{R})}{\partial\lambda}g_{ref}(\lambda,\mathbf{R}). \qquad \text{(C27)}$$

Finally, combining Eqs. (C22)–(C24) and (C27) leads to

$$\frac{\rho_I}{2}\int d\mathbf{R}\frac{\partial g_{ref}(\lambda_{eff},\mathbf{R})}{\partial\lambda}[\Phi(\mathbf{R})-\Phi_{ref}(\lambda_{eff},\mathbf{R})]=0, \qquad \text{(C28)}$$

which is simply Eq. (30).

[1] S. Ichimaru, *Statistical Plasma Physics, Vol. II: Condensed Plasmas* (Addison-Wesley, New York, 1994).
[2] I. Krisch and H.J. Kunze, Phys. Rev. E **58**, 6557 (1998).
[3] A.W. DeSilva and J.D. Katsouros, Phys. Rev. E **57**, 5945 (1998).
[4] J.F. Benage, W.R. Shanahan, and M.S. Murillo, Phys. Rev. Lett. **83**, 2953 (1999).
[5] A. Ng, D. Parfeniuk, P. Celliers, L. DaSilva, R.M. More, and Y.T. Lee, Phys. Rev. Lett. **57**, 1595 (1986).
[6] A. Ng, P. Celliers, A. Forsman, R.M. More, Y.T. Lee, F. Perrot, M.W.C. Dharma-wardana, and G.A. Rinker, Phys. Rev. Lett. **72**, 3351 (1994).
[7] Good reviews are found in the special issue of Contrib. Plasma Phys. **41** 2001.
[8] P. Renaudin, C. Blancard, G. Faussurier, and P. Noiret, Phys. Rev. Lett. **88**, 215001 (2002).
[9] P. Renaudin, C. Blancard, J. Clérouin, G. Faussurier, P. Noiret, and V. Recoules, Phys. Rev. Lett. **91**, 075002 (2003), and references therein.
[10] SESAME: The Los Alamos National Laboratory Equation of State Database, Report No. LA-UR-92-3407, edited by S.P. Lyon and J. Johnson, Group T-1 (unpublished).
[11] K. Trainor, in *Handbook of Material Properties Data Bases*, edited by W. Huebner (Los Alamos National Laboratory, Los Alamos, 1984), Vol. Ic, p. 3712.
[12] F. Perrot, M.W.C. Dharma-Wardana, and J. Benage, Phys. Rev. E **65**, 046414 (2002).
[13] R.W. Lee, H.A. Baldis, R.C. Cauble, O.L. Landen, J.S. Wark, A. Ng, S.J. Rose, C. Lewis, D. Riley, J.-C. Gauthier, and P. Audebert, Laser Part. Beams **20**, 527 (2002).
[14] F. Perrot and M.W.C. Dharma-Wardana, Phys. Rev. E **52**, 5352 (1995), and references therein.
[15] R.P. Feynman, N. Metropolis, and E. Teller, Phys. Rev. **75**, 1561 (1949).
[16] D.A. Liberman, Phys. Rev. B **20**, 4981 (1979).
[17] D. Ofer, E. Nardi, and Y. Rosenfeld, Phys. Rev. A **38**, 5801 (1988).
[18] J.M. Ziman, *Principle of Theory of Solids* (Cambridge University Press, Cambridge, 1972).
[19] R.P. Feynman, *Statistical Mechanics* (Addison-Wesley, New York, 1972).
[20] S. Kiyokawa, J. Phys. Soc. Jpn. **64**, 4708 (1995).
[21] N.W. Ashcroft and D. Stroud, Solid State Phys. **33**, 1 (1978).
[22] J.-P. Hansen and I.R. McDonald, *Theory of Simple Liquids*, 2nd ed. (Academic Press, London, 1986).
[23] G. Faussurier and M.S. Murillo, Phys. Rev. E **67**, 046404 (2003).
[24] H. Iyetomi and S. Ichimaru, Phys. Rev. A **34**, 433 (1986).
[25] J.P. Perdew and Y. Wang, Phys. Rev. **45**, 13244 (1992).
[26] R.G. Gordon and Y.S. Kim, J. Chem. Phys. **56**, 3122 (1972).
[27] W.H. Press, S.A. Teukolski, W.T. Vetterling, and B.P. Flannery, *Numerical Recipes in Fortran: the Art of Scientific Computing*, 2nd ed. (Cambridge University Press, New York, 1992).
[28] Y. Rosenfeld, Phys. Rev. A **15**, 2545 (1977).
[29] Y. Rosenfeld, J. Phys.: Condens. Matter **11**, 5415 (1999).
[30] F. Perrot and M.W.C. Dharma-wardana, Phys. Rev. A **36**, 238 (1987).
[31] R.M. More, K.H. Warren, D.A. Young, and G.B. Zimmerman, Phys. Fluids **31**, 3059 (1988).
[32] J.W. Jeong, I.H. Lee, and K.J. Chang, Phys. Rev. B **59**, 329 (1999).
[33] J.P. Perdew and A. Zunger, Phys. Rev. B **23**, 5048 (1981).
[34] A.B. Alchagirov, J.P. Perdew, J.C. Boettger, R.C. Albers, and C. Fiolhais, Phys. Rev. B **63**, 224115 (2001).
[35] W.J. Nellis, J.A. Moriarty, A.C. Mitchell, M. Ross, R.G. Dandrea, N.W. Ashcroft, N.C. Holmes, and G.R. Gathers, Phys. Rev. Lett. **60**, 1414 (1988).
[36] R.G. Greene, H. Luo, and A.L. Ruoff, Phys. Rev. Lett. **73**, 2075 (1994).
[37] B.F. Rozsnyai, J.R. Albritton, D.A. Young, V.N. Sonnad, and D.A. Liberman, Phys. Lett. A **291**, 226 (2001), and references therein.
[38] Y. Zeldovich and Y. Rayzer, *Physics of Shock Waves and High-Temperature Hydrodynamics Phenomena* (Academic Press, New York, 1966).
[39] S. Kuhlbrodt and R. Redmer, J. Phys. A **36**, 6027 (2003).
[40] R. Redmer, Phys. Rev. E **59**, 1073 (1999).
[41] S. Kuhlbrodt and R. Redmer, Phys. Rev. E **62**, 7191 (2000).
[42] S.H. Glenzer, G. Gregori, R.W. Lee, F.J. Rogers, S.W. Pollaine, and O.L. Landen, Phys. Rev. Lett. **90**, 175002 (2003).
[43] F.J. Rogers and D.A. Young, Phys. Rev. E **56**, 5876 (1997).
[44] F.J. Rogers, Phys. Plasmas **7**, 51 (2000).
[45] F. Perrot, Phys. Rev. E **47**, 570 (1993).
[46] J.W. Negele and H. Orland, *Quantum Many-Particle Systems* (Addison-Wesley, New York, 1988).